*Desalination and Water Treatment*
www.deswater.com

doi: 10.1080/19443994.2015.1067838

57 (2016) 14973–14985
July

Taylor & Francis
Taylor & Francis Group

# Modeling of decolorization of synthetic reactive dyestuff solutions with response surface methodology by a rapid and efficient process of ultrasound-assisted ozone oxidation

Musa Buyukada

*Department of Environmental Engineering, Abant Izzet Baysal University, Bolu, Turkey, Tel. +90 374 254 1000; Fax: +90 374 254 4548; email: musabuyukada@hotmail.com*

Received 28 January 2015; Accepted 23 June 2015

ABSTRACT

The present study investigates the results of decolorization of Malachite Green (MG), Reactive Black 5 (RB5), and Reactive Yellow 145 (RY145) in aqueous solutions based on a rapid and novel process of ultrasound-assisted ozonation. A Placket–Burman design (PBD) as a factorial design was used to quantify and screen the significant effects of the seven factors on decolorization efficiency: temperature (°C), initial pH, probe position (height from bottom of reactor, mm), reaction time (min), ozone concentration (g/L), mixing speed (rpm), and ultrasonic power (W). Probe position and mixing speed were not found as significant after considering the regression and ANOVA results of PBD. A Box–Behnken design (BBD) as a kind of response surface methodology, with remaining five factors at three levels was set to demonsrate the interactions. The best-fit multi non-linear regression (MNLR) models were derived by using the results of BBD. According to BBD, the maximum decolorization efficiency of 99.31, 99.86, and 99.52% were obtained consistently at the lowest initial pH of 2, the highest reaction time of 30 min, and ozone concentration of 0.15 g/L for MG, RB5, and RY145, respectively. The best-fit MNLR models were cross-validated ($R^2_{pred}$) accounting for 81.02–88.25% and were expressed ($R^2_{adj}$) accounting for 93.01–95.70% of variation in decolorization efficiency.

*Keywords:* Decolorization; RSM, Anova; Non-linear regression; Ultrasonic irradiation; Ozone oxidation

## 1. Introduction

Synthetic dyestuffs are commonly used in textile industries and discharging of these synthetic wastewaters causes important environmental pollutantion and harm to well-being of humans [1]. There are more than 10,000 commercially available dyes, most of which are difficult to biodegrade due to their complex aromatic molecular structure [2]. Therefore, removal of dyes before discharging these wastewaters is environmentally and economically of great importance [3]. Many researchers have used traditional treatment methods for decolorization of reactive dyestuff aqueous solution of such wastewaters such as chemical coagulation and/or ozonation [4,5], electrochemical treatment [6,7], biological treatment [8], and adsorption [1–9]. However, these common treatment methods have not been efficient enough for decolorization of reactive dyes aqueous solutions [9–11].

Nowadays, advanced oxidation processes (AOPs) such as Fenton, electro-Fenton, ozonation, catalytic ozone oxidation, ultrasonic irradiation, and photocatalytic degradation have also gained an increasing importance in the treatment and decolorization of dye solutions from wastewaters [12,13]. Especially, there exists recently increased interest in the applications of sonolysis and ozone treatments to wastewaters contaminated with reactive dyes [14–17]. Ultrasound (US) causes a cycle that follows the formation, growth, and sudden collapse of acoustic cavitation-induced microbubbles in an irradiated liquid and mixture medium becomes highly localized temperatures (up to 4,200 K) and pressures (975 bars) [12,13,18–20]. Although most organic compounds can be decomposed by the ultrasonic irradiation, much effort has been devoted to accelerate the decomposition rates that are still slow for practical uses [21].

Ozone has frequently been used for decolorization of textile wastewater, but high cost of ozone production and low utilization of ozone mass transfer have been limited industrial applications of ozonation ($O_3$) [22]. A method to enhance ozonation reaction may be through the usage of US and a novel combined technology might be also further useful and charming [22,23]. Collocation of US with $O_3$ is able to provide possible AOPs that $O_3$ is decomposed in vapor phase of a sudden cavitation bubble by US [23]:

$$O_{3(g)} \overset{US}{\rightarrow} O_{2(g)} + O(P^3)_{(g)} \quad (1)$$

$$O(P^3)_{(g)} + H_2O \rightarrow 2^{\cdot}OH_{(}g) \quad (2)$$

These decomposition reactions, where P indicates pollutants, occur in the gas phase and the product of reaction migrate to the interfacial sheath of the bubble and US has been demonsrated to increase the mass transfer of ozone to solution by means of increasing volumetric mass-transfer coefficient [23]. Acidic mixture medium with low concentration of $O_3$ can lead decolorization efficiency to increase; but in basic medium $O_3$, decomposition reactions occur as shown below [24]:

$$O_3 + OH^- \rightarrow HO_2^{\cdot} + O_2^{\cdot -} \quad (3)$$

$$HO_2^{\cdot} \leftrightarrow H^+ + O_2^{\cdot -} \quad (4)$$

$$O_3 + O_2^{\cdot -} \rightarrow O_3^{\cdot -} + O_2 \quad (5)$$

$$O_3^{\cdot -} + H^+ \leftrightarrow HO_3^{\cdot} \quad (6)$$

$$HO_3^{\cdot} \rightarrow HO^{\cdot} + O_2 \quad (7)$$

$$HO_4^{\cdot} \rightarrow HO_2^{\cdot} + O_2^{\cdot} \quad (8)$$

$$HO_4^{\cdot} + HO_3^{\cdot} \rightarrow H_2O_2 + O_3 + O_2 \quad (9)$$

$$HO_4^{\cdot} + HO_4^{\cdot} \rightarrow H_2O_2 + 2O_3 \quad (10)$$

So, basic solution needs more $O_3$ input. Collocation of US with $O_3$ has been widely used for the destruction of aqueous pollutants [22–24].

In the present study, decolorization of Malachite Green (MG), Reactive Black 5 (RB5), and Reactive Yellow 145 (RY145) aqueous solutions by ultrasound-assisted ozonation was explored to quantify the effects of temperature (°C), initial pH, probe height (from bottom of reactor, mm), reaction time (min), ozone concentration (g/L), mixing speed (rpm), and ultrasonic power (W) on decolorization efficiency.

## 2. Materials and methods

### 2.1. Chemicals and materials

Malachite Green (MG, C.I. No: 510-13-04, analytical grade) triphenylmethane dyestuff, Reactive Black 5 (RB5, C.I. No: 17095-24-8), and Reactive Yellow 145 (RY145, C.I. No: 93050-80-7) were obtained from a local textile factory, Corlu, Turkey and used in experiments without any purification. Characteristic and chemical properties of dyestuffs are given in Table 1.

### 2.2. Reactive dyestuff solution

The stock solutions of reactive dyestuffs were prepared in a constant concentration of 1.0 g/L and then diluted to appropriate concentrations. Working solutions of the desired concentrations were obtained using successive dilutions and the initial pH of each solution was adjusted to the required value with 1.0 M of $H_2SO_4$ and NaOH solutions before experiments.

Table 1
Properties of dyestuffs (A: Absorbance, IU; C: Concentration of dyestuff, mg/L)

| Dyestuff name | Malachite Green (MG) | Reactive Black 5 (RB5) | Reactive Yellow 145 (RY145) |
|---|---|---|---|
| Chemical formula | $C_{23}H_{25}ClN_2$ | $C_{22}H_{16}N_2O_{11}S_3Na_2$ | $C_{28}H_{20}ClN_9O_{16}S_5Na_4$ |
| Molecular weight (g/mol) | 364.92 | 626.549 | 1026.26 |
| $\lambda_{max}$ (nm) | 617 | 595 | 520 |
| Calibration equation | $A = 0.0197*C_{MG}$ | $A = 0.0181*C_{RB5}$ | $A = 0.0169*C_{RY145}$ |
| $R^2$ | 0.98 | 0.99 | 0.98 |
| $p$ (<0.05) | 0.001 | 0.001 | 0.001 |

### 2.3. Experimental procedure

Decolorization experiments were carried out following the experimental setup as shown in Fig. 1. The experiments were effectuated in a cylindrical jacketed vessel (reactor) made of Pyrex with a height of 110 cm and a diameter of 5 cm that put on a mechanical stirrer (IKA RW 20, Kutay Group, Turkey) which stirred the mixture at various agitation speed range of 100–200 rpm. A titanium probe transducer, 8 mm in diameter, was set in reactor operating at a frequency of 40 kHz and an ultrasonic generetor (FS-300, China) was used for sonolysis that has a sonolytic power range of 50–500 W. Ozone was produced from a generator with a gas flowmeter (TKZ-H-6G, Tekazone, Turkey) and flow rate of gas ozone into reactor was controlled by flow meter. Total reactive dyestuff solution volume was determined 2000 mL by considering similar studies [12,13,18–24]. The experiments were repeated according to schedule of experimental design.

### 2.4. Dye analysis

The solutions were analyzed at predetermined reaction time intervals for the final concentration of MG, RB5, and RY145 using a UV/vis spectrophotometer (SHIMADZU UV-2100, Biomerieux, France) at a wave length of 617, 595 and 520 nm for the maximum absorbance value, respectively. Decolorization efficiency (DE, %) at any time was estimated as follows [2,9,12,24]:

$$\text{Decolorization efficiency}(\text{DE}, \%) = \frac{A_0 - A_t}{A_0} \times 100 \quad (11)$$

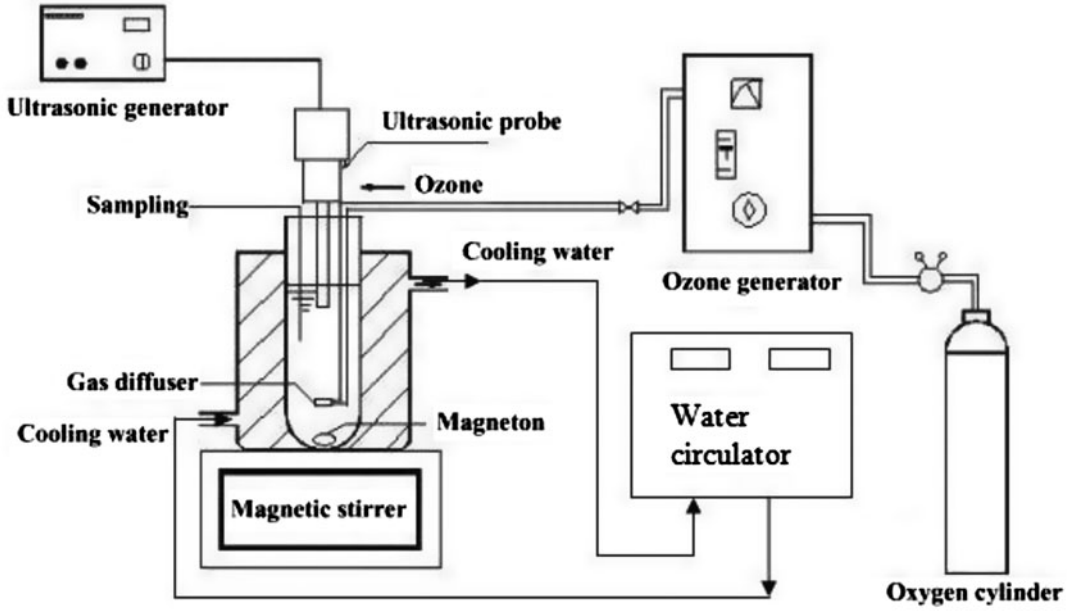


Fig. 1. A schematic view of the experimental setup used in the present study.

where $A_0$ is initial absorbance value and $A_t$ is measured absorbance values of the samples at a specified interval during the reaction. Dyestuff concentration after each experiment was calculated using the best-fit calibration graph (Table 1). Also isoelectric points ($pH_{iep}$) of MG, RB5, and RY145 were measured using a titration method, respectively.

### 2.5. Statistical analyses

In the experiments, Placket–Burman design (PBD) was used to state the significant effects of seven explanatory variables on decolorization efficiency. In PBD, explanatory variables were varied two levels of minimum (−) and maximum (+) (Table 2). PBD requires 12 runs were employed with a replicate and thus a total of 24 runs were done. Considering the results of PBD (Table 3), probe position (height from bottom of reactor) and mixing speed were eleminated and a Box–Behnken design (BBD) with remains five factors at three levels (−, 0, +) was set to apply response surface motodology (RSM) given in Table 4.

Each factors was coded as minimum (−), median (0), and maximum (+), respectively at the ranges determined by the preliminary experiments where temperature ($x_1$) of 20–60°C, initial pH ($x_2$) of 2.0–8.0, reaction time ($x_3$) of 10–30 min, ultrasonic power ($x_4$) of 86–344 W, and ozone concentration ($x_5$) of 0.05–0.15 g/L. Explanatory variable (factor) was coded $x_i$ according to relationship given in (12):

$$X_i = \frac{x_i - x_o}{\Delta x} \times 100 \quad (12)$$

where ΔX is the step change value, also $X_i$, $x_i$ and $x_o$ are the coded value, the actual value and the center point actual value of explanatory variable, respectively. The total run of experiment with five factors at three levels was determined as 46 by RSM and the response variable was decolorization efficiency (DE, %).

Anderson–Darling test and the four plots about normal distribution were applied to check the assumptions of normality, constant variance, and autocorrelation, respectively, prior to the implementation of the parametric tests of analysis of variance (ANOVA) and multiple nonlinear regressions (MNLR). Tukey's multiple comparisons at a confidence interval of 95% were used to detect the significant differences in decolorization efficiency among the explanatory variables following ANOVA. Best-fit MNLR models were built to explicate the efficacy of explanatory factors and their interactions for the prediction of the response variable (decolorization efficiency).

The best subset procedure was used to choose the best-fit MNLR models with the highest goodness-of-fit, and the highest predictive power which was measured by adjusted coefficient of determination ($R^2_{adj}$) and coefficient of determination based on leave-one-out cross-validation ($R^2_{CV}$). Variance inflation factor (VIF) for multicollinearity and Durbin–Watson (D–W) statistics for autocorrelation were reported for the best-fit MNLR models. Design of experiment and all the statistical analyses were performed using Minitab 16.1 (Minitab, Inc., State Collage, PA).

Table 2
Plackett–Burmann design (PBD) for determination of main effects of explanatory variables on decolorization efficiency of MG, RB5, and RY145

| | Coded variables | | | | | | | Experimental predictors | | | | | | | Response variables | | |
|---|---|---|---|---|---|---|---|---|---|---|---|---|---|---|---|---|---|
| Run | $x_1$ | $x_2$ | $x_3$ | $x_4$ | $x_5$ | $x_6$ | $x_7$ | $x_1$ (°C) | $x_2$ (pH) | $x_3$ (mm) | $x_4$ (min) | $x_5$ (g/L) | $x_6$ (rpm) | $x_7$ (W) | MG Exp. | RB5 Exp. | RY145 Exp. |
| 1 | − | − | − | − | − | − | − | 30 | 2.0 | 50 | 10 | 0.05 | 100 | 86 | 14.6 | 10.33 | 12.28 |
| 2 | + | + | − | + | + | − | + | 30 | 8.0 | 50 | 30 | 0.15 | 100 | 344 | 35.1 | 33.06 | 33.21 |
| 3 | + | − | + | + | − | + | − | 30 | 8.0 | 200 | 30 | 0.05 | 200 | 86 | 17.1 | 20.06 | 18.89 |
| 4 | + | − | + | − | − | − | + | 30 | 8.0 | 200 | 10 | 0.05 | 100 | 344 | 21.4 | 20.66 | 20.41 |
| 5 | − | − | + | + | + | − | + | 40 | 2.0 | 200 | 30 | 0.15 | 100 | 344 | 21.7 | 26.10 | 23.26 |
| 6 | − | + | + | − | + | − | − | 30 | 2.0 | 200 | 10 | 0.15 | 100 | 86 | 17.6 | 18.20 | 17.31 |
| 7 | + | + | − | + | − | − | − | 20 | 8.0 | 50 | 30 | 0.05 | 100 | 86 | 28.7 | 30.73 | 29.89 |
| 8 | − | + | + | + | − | + | + | 30 | 2.0 | 200 | 30 | 0.05 | 200 | 344 | 79.1 | 72.46 | 71.56 |
| 9 | + | − | − | − | + | + | + | 30 | 8.0 | 50 | 10 | 0.15 | 200 | 344 | 10.6 | 8.96 | 9.12 |
| 10 | + | + | + | − | + | + | − | 30 | 8.0 | 200 | 10 | 0.15 | 200 | 86 | 15.1 | 14.50 | 15.21 |
| 11 | − | − | − | + | + | + | − | 30 | 2.0 | 50 | 30 | 0.15 | 200 | 86 | 12.8 | 12.06 | 11.76 |
| 12 | − | + | − | − | − | + | + | 30 | 2.0 | 50 | 10 | 0.05 | 200 | 86 | 52.4 | 59.03 | 57.31 |

Table 3
Regression and ANOVA results of PBD

| Dyestuff | Source | DF | Seq SS | Adj SS | Adj MS | $F$ | $p$ (<0.005) | VIF |
|---|---|---|---|---|---|---|---|---|
| Malachite Green (MG) | Constant | 1 | 4292.36 | 4292.36 | 613.19 | 16.67 | 0.008 | |
| | $x_1$ | 1 | 410.67 | 410.67 | 410.67 | 11.17 | 0.029 | 1.001 |
| | $x_2$ | 1 | 1404 | 1404 | 1404 | 38.18 | 0.003 | 1.001 |
| | $x_3$ | 1 | 26.4 | 26.4 | 26.4 | 0.72 | 0.445 | 1.001 |
| | $x_4$ | 1 | 328.65 | 328.65 | 328.65 | 8.94 | 0.045 | 1.001 |
| | $x_5$ | 1 | 840.01 | 840.01 | 840.01 | 22.84 | 0.009 | 1.001 |
| | $x_6$ | 1 | 192 | 192 | 192 | 5.22 | 0.084 | 1.001 |
| | $x_7$ | 1 | 1090.61 | 1090.61 | 1090.61 | 29.66 | 0.006 | 1.001 |
| | $R^2 = 0.9669$; $R^2_{adj} = 0.9089$; $R^2_{pred} = 0.7018$; S = 6.06; Press = 1323.9 | | | | | | | |
| Reactive Black 5 (RB5) | Constant | 1 | 4292.36 | 4292.36 | 613.19 | 16.67 | 0.008 | |
| | $x_1$ | 1 | 410.79 | 410.79 | 410.67 | 11.17 | 0.029 | 1.001 |
| | $x_2$ | 1 | 1404.22 | 1404.22 | 1404 | 38.18 | 0.003 | 1.001 |
| | $x_3$ | 1 | 26.43 | 26.43 | 26.4 | 0.72 | 0.527 | 1.001 |
| | $x_4$ | 1 | 328.55 | 328.55 | 328.65 | 8.94 | 0.045 | 1.001 |
| | $x_5$ | 1 | 839.85 | 839.85 | 840.01 | 22.84 | 0.009 | 1.001 |
| | $x_6$ | 1 | 191.92 | 191.92 | 192 | 5.22 | 0.091 | 1.001 |
| | $x_7$ | 1 | 1090.42 | 1090.42 | 1090.61 | 29.66 | 0.006 | 1.001 |
| | $R^2 = 0.9599$; $R^2_{adj} = 0.8991$; $R^2_{pred} = 0.6789$; S = 8.12; Press = 2127.8 | | | | | | | |
| Reactive Yellow 145 (RY145) | Constant | 1 | 4292.36 | 4292.36 | 613.19 | 16.67 | 0.008 | |
| | $x_1$ | 1 | 410.79 | 410.79 | 410.67 | 11.17 | 0.029 | 1.001 |
| | $x_2$ | 1 | 1404.22 | 1404.22 | 1404 | 38.18 | 0.003 | 1.001 |
| | $x_3$ | 1 | 26.43 | 26.43 | 26.4 | 0.72 | 0.493 | 1.001 |
| | $x_4$ | 1 | 328.55 | 328.55 | 328.65 | 8.94 | 0.041 | 1.001 |
| | $x_5$ | 1 | 839.85 | 839.85 | 840.01 | 22.84 | 0.009 | 1.001 |
| | $x_6$ | 1 | 191.92 | 191.92 | 192 | 5.22 | 0.089 | 1.001 |
| | $x_7$ | 1 | 1090.42 | 1090.42 | 1090.61 | 29.66 | 0.006 | 1.001 |
| | $R^2 = 0.9781$; $R^2_{adj} = 0.9124$; $R^2_{pred} = 0.7108$; S = 5.82; Press = 1087.1 | | | | | | | |

## 3. Results and discussion

### 3.1. Explication of experimental results

The experimantal results were analyzed by the response variable of decolorization efficiency (DE, %) using Minitab 16.1. Normal distribution graphs (Fig. 2) showed that there was a normal distribution between experimental data and the necessary assumptions for statistical analysis were met for ANOVA and MNLR. ANOVA results of PBD showed that five of seven explanatory variables were significantly effective on decolorization efficiency (Table 3).

$$Y_1 = 27.183 - 5.85x_1 + 10.817x_2 + 1.483x_3 + 5.233x_4 - 8.367x_5 + 4.001x_6 + 9.533x_7 \quad (13)$$

$$Y_2 = 29.556 - 7.15x_1 + 12.311x_2 + 1.133x_3 + 5.293x_4 - 10.361x_5 + 4.031x_6 + 10.813x_7 \quad (14)$$

$$Y_3 = 25.371 - 6.89x_1 + 11.471x_2 + 1.033x_3 + 4.9973x_4 - 9.352x_5 + 4.028x_6 + 11.007x_7 \quad (15)$$

Eqs. (13)–(15) were derived as the multi linear regression (MLR) models of PBD. Explanatory variables of $x_1$, $x_2$, $x_3$, $x_4$, $x_5$, $x_6$, and $x_7$ correspond to temperature, initial pH, height of probe (from bottom of reactor), reaction time, ozone concentration, shaking speed, and ultrasonic power, response variables of predicted decolorization efficiencies of $Y_1$, $Y_2$, and $Y_3$ correspond to MG, RB5, and RY145, respectively.

$$Y_1 = -81.04 - 1.9887x_1 + 25.15x_2 + 5.753x_3 + 0.8135x_4 + 934.1x_5 + 0.23833x_1^2 - 0.005x_2^2 - 0.3826x_2x_3 - 0.010837x_2x_4 - 112.47x_2x_5 - 0.003031x_3x_4 - 17.14x_3x_5 \quad (16)$$

Table 4
Experimental schedule and predicted results of Box–Behnken design (BBD) for decolorization efficiency of MG, RB5, and RY145

| | Coded variables | | | | | Experimental predictors | | | | | Response variable | | | | | |
|---|---|---|---|---|---|---|---|---|---|---|---|---|---|---|---|---|
| | | | | | | | | | | | MG | | RB5 | | RY145 | |
| Run | $x_1$ | $x_2$ | $x_3$ | $x_4$ | $x_5$ | $x_1$ (°C) | $x_2$ (pH) | $x_3$ (min) | $x_4$ (W) | $x_5$ (g/L) | Exp. | Pred. | Exp. | Pred. | Exp. | Pred. |
| 1 | 0 | 0 | − | 0 | − | 40 | 5.0 | 10 | 172 | 0.05 | 41.28 | 40.29 | 41.76 | 43.58 | 41.29 | 43.84 |
| 2 | 0 | + | 0 | 0 | − | 40 | 8.0 | 20 | 172 | 0.05 | 73.21 | 72.63 | 75.34 | 74.28 | 74.63 | 76.28 |
| 3 | 0 | 0 | + | − | 0 | 40 | 5.0 | 30 | 86 | 0.10 | 88.89 | 90.93 | 90.22 | 90.45 | 90.93 | 89.14 |
| 4 | 0 | 0 | − | − | 0 | 40 | 5.0 | 10 | 86 | 0.10 | 50.41 | 55.49 | 49.73 | 50.06 | 52.49 | 49.77 |
| 5 | + | 0 | + | 0 | 0 | 60 | 2.0 | 30 | 172 | 0.10 | 93.26 | 88.52 | 99.86 | 95.03 | 99.52 | 95.24 |
| 6 | 0 | − | 0 | + | 0 | 40 | 2.0 | 20 | 344 | 0.10 | 77.31 | 80.76 | 69.55 | 76.15 | 70.76 | 74.57 |
| 7 | − | − | 0 | 0 | 0 | 20 | 2.0 | 20 | 172 | 0.10 | 79.89 | 81.14 | 80.51 | 81.35 | 80.14 | 81.23 |
| 8 | 0 | 0 | 0 | 0 | 0 | 40 | 5.0 | 20 | 172 | 0.10 | 71.56 | 72.33 | 67.74 | 71.08 | 71.33 | 70.11 |
| 9 | 0 | 0 | 0 | + | − | 40 | 5.0 | 20 | 344 | 0.05 | 69.12 | 62.54 | 65.39 | 66.86 | 64.54 | 67.06 |
| 10 | 0 | − | − | 0 | 0 | 40 | 2.0 | 10 | 172 | 0.10 | 45.21 | 40.76 | 44.67 | 44.85 | 40.76 | 43.86 |
| 11 | 0 | + | 0 | + | 0 | 40 | 8.0 | 20 | 344 | 0.10 | 58.76 | 62.35 | 60.23 | 58.43 | 60.35 | 57.25 |
| 12 | 0 | − | + | 0 | 0 | 40 | 2.0 | 30 | 172 | 0.10 | 99.31 | 92.71 | 98.77 | 98.15 | 95.80 | 98.34 |
| 13 | 0 | 0 | − | 0 | + | 40 | 5.0 | 10 | 172 | 0.15 | 71.77 | 72.12 | 75.19 | 72.53 | 77.14 | 73.65 |
| 14 | 0 | 0 | 0 | 0 | 0 | 40 | 5.0 | 20 | 172 | 0.10 | 69.42 | 68.15 | 67.74 | 71.08 | 70.95 | 70.11 |
| 15 | 0 | − | 0 | 0 | + | 40 | 2.0 | 20 | 172 | 0.15 | 92.60 | 91.56 | 93.81 | 95.66 | 94.76 | 95.62 |
| 16 | + | 0 | − | 0 | 0 | 40 | 5.0 | 10 | 172 | 0.10 | 61.22 | 53.73 | 61.17 | 61.91 | 58.73 | 59.67 |
| 17 | 0 | + | 0 | 0 | + | 40 | 8.0 | 20 | 172 | 0.15 | 48.21 | 50.11 | 51.10 | 51.36 | 50.11 | 50.91 |
| 18 | 0 | + | 0 | − | 0 | 40 | 8.0 | 20 | 86 | 0.10 | 63.11 | 61.88 | 60.04 | 64.34 | 61.88 | 63.44 |
| 19 | 0 | 0 | + | 0 | + | 40 | 5.0 | 30 | 172 | 0.15 | 86.34 | 91.77 | 80.81 | 84.91 | 81.77 | 84.14 |
| 20 | 0 | 0 | 0 | 0 | 0 | 40 | 5.0 | 20 | 172 | 0.10 | 71.12 | 68.92 | 67.74 | 71.08 | 68.09 | 70.11 |
| 21 | − | 0 | 0 | 0 | − | 20 | 5.0 | 20 | 172 | 0.05 | 82.45 | 86.37 | 75.35 | 78.28 | 76.37 | 78.72 |
| 22 | − | 0 | 0 | 0 | + | 20 | 5.0 | 20 | 172 | 0.15 | 90.56 | 89.65 | 89.69 | 90.88 | 89.65 | 89.94 |
| 23 | 0 | 0 | 0 | + | + | 30 | 5.0 | 20 | 344 | 0.15 | 80.19 | 74.64 | 76.57 | 79.91 | 74.64 | 79.11 |
| 24 | + | 0 | 0 | 0 | − | 60 | 5.0 | 20 | 172 | 0.05 | 75.27 | 82.11 | 78.33 | 73.84 | 82.11 | 74.33 |
| 25 | 0 | 0 | + | 0 | − | 40 | 5.0 | 30 | 172 | 0.05 | 90.13 | 93.95 | 95.40 | 90.24 | 93.95 | 93.36 |
| 26 | 0 | 0 | + | + | 0 | 40 | 5.0 | 30 | 344 | 0.10 | 79.98 | 80.46 | 79.82 | 81.83 | 80.46 | 81.86 |
| 27 | 0 | 0 | 0 | − | + | 40 | 5.0 | 20 | 86 | 0.15 | 79.06 | 70.73 | 74.36 | 76.43 | 70.73 | 75.27 |
| 28 | 0 | + | − | 0 | 0 | 40 | 8.0 | 10 | 172 | 0.10 | 66.59 | 60.35 | 60.09 | 59.06 | 60.35 | 59.28 |
| 29 | + | + | 0 | 0 | 0 | 60 | 8.0 | 20 | 172 | 0.10 | 67.54 | 69.29 | 69.50 | 66.56 | 69.29 | 66.86 |
| 30 | 0 | 0 | 0 | 0 | 0 | 40 | 5.0 | 20 | 172 | 0.10 | 71.13 | 69.26 | 67.74 | 71.08 | 68.06 | 70.11 |
| 31 | 0 | 0 | − | + | 0 | 40 | 5.0 | 10 | 344 | 0.10 | 63.23 | 63.74 | 61.04 | 63.17 | 63.74 | 61.21 |
| 32 | 0 | 0 | 0 | 0 | 0 | 40 | 5.0 | 20 | 172 | 0.10 | 72.12 | 74.26 | 67.74 | 71.08 | 67.26 | 70.11 |
| 33 | 0 | + | + | 0 | 0 | 40 | 8.0 | 30 | 172 | 0.10 | 67.13 | 66.44 | 65.25 | 64.80 | 66.44 | 64.81 |
| 34 | − | + | 0 | 0 | 0 | 20 | 8.0 | 20 | 172 | 0.10 | 75.89 | 70.84 | 72.34 | 75.61 | 70.84 | 73.07 |
| 35 | 0 | − | 0 | − | 0 | 40 | 2.0 | 20 | 86 | 0.10 | 65.34 | 65.76 | 68.83 | 65.75 | 71.76 | 64.22 |
| 36 | + | 0 | 0 | − | 0 | 60 | 5.0 | 20 | 86 | 0.10 | 78.45 | 79.64 | 81.90 | 81.06 | 79.64 | 79.36 |
| 37 | − | 0 | 0 | − | 0 | 20 | 5.0 | 20 | 86 | 0.10 | 76.98 | 74.76 | 74.57 | 77.76 | 74.76 | 75.40 |
| 38 | + | − | 0 | 0 | 0 | 60 | 2.0 | 20 | 172 | 0.10 | 79.18 | 80.37 | 79.45 | 79.95 | 80.37 | 76.80 |
| 39 | − | 0 | + | 0 | 0 | 20 | 5.0 | 30 | 172 | 0.10 | 97.02 | 94.01 | 92.75 | 96.65 | 94.01 | 95.00 |
| 40 | − | 0 | 0 | + | 0 | 20 | 5.0 | 20 | 344 | 0.10 | 88.83 | 84.58 | 84.30 | 88.53 | 84.58 | 86.76 |
| 41 | + | 0 | 0 | 0 | + | 60 | 5.0 | 20 | 172 | 0.15 | 85.82 | 83.54 | 82.82 | 84.87 | 85.54 | 83.69 |
| 42 | 0 | 0 | 0 | 0 | 0 | 40 | 5.0 | 20 | 172 | 0.10 | 71.11 | 67.74 | 67.74 | 71.08 | 67.74 | 70.11 |
| 43 | 0 | 0 | 0 | − | − | 40 | 5.0 | 20 | 86 | 0.05 | 67.47 | 64.15 | 66.70 | 65.86 | 64.15 | 66.74 |
| 44 | 0 | − | 0 | 0 | − | 40 | 2.0 | 20 | 172 | 0.05 | 50.12 | 45.97 | 50.74 | 49.11 | 51.97 | 49.68 |
| 45 | + | 0 | 0 | + | 0 | 60 | 5.0 | 20 | 344 | 0.10 | 77.24 | 70.90 | 73.07 | 74.77 | 70.90 | 72.15 |
| 46 | − | 0 | − | 0 | 0 | 20 | 5.0 | 10 | 86 | 0.10 | 72.18 | 70.33 | 71.18 | 70.73 | 70.33 | 70.55 |

$$Y_2 = -64.87 - 2.026x_1 + 30.344x_2 + 4.6701x_3 + 0.12313x_4 + 1046.7x_5 + 0.026x_1^2 - 0.4104x_2^2 + 0.025x_3^2 + 968.8x_4^2 - 0.0011335x_1x_4 - 0.35344x_2x_3 - 112.183x_2x_5 - 0.003x_3x_4 - 24.01x_3x_5 \quad (17)$$

$$Y_3 = -75.32 - 1.9221x_1 + 21.042x_2 + 4.9811x_3 + 0.14717x_4 + 1084x_5 + 0.025587x_1^2 - 0.4679x_2^2 - 0.3547x_2x_3 - 112.18x_2x_5 - 0.003172x_3x_4 - 24.015x_3x_5 \quad (18)$$

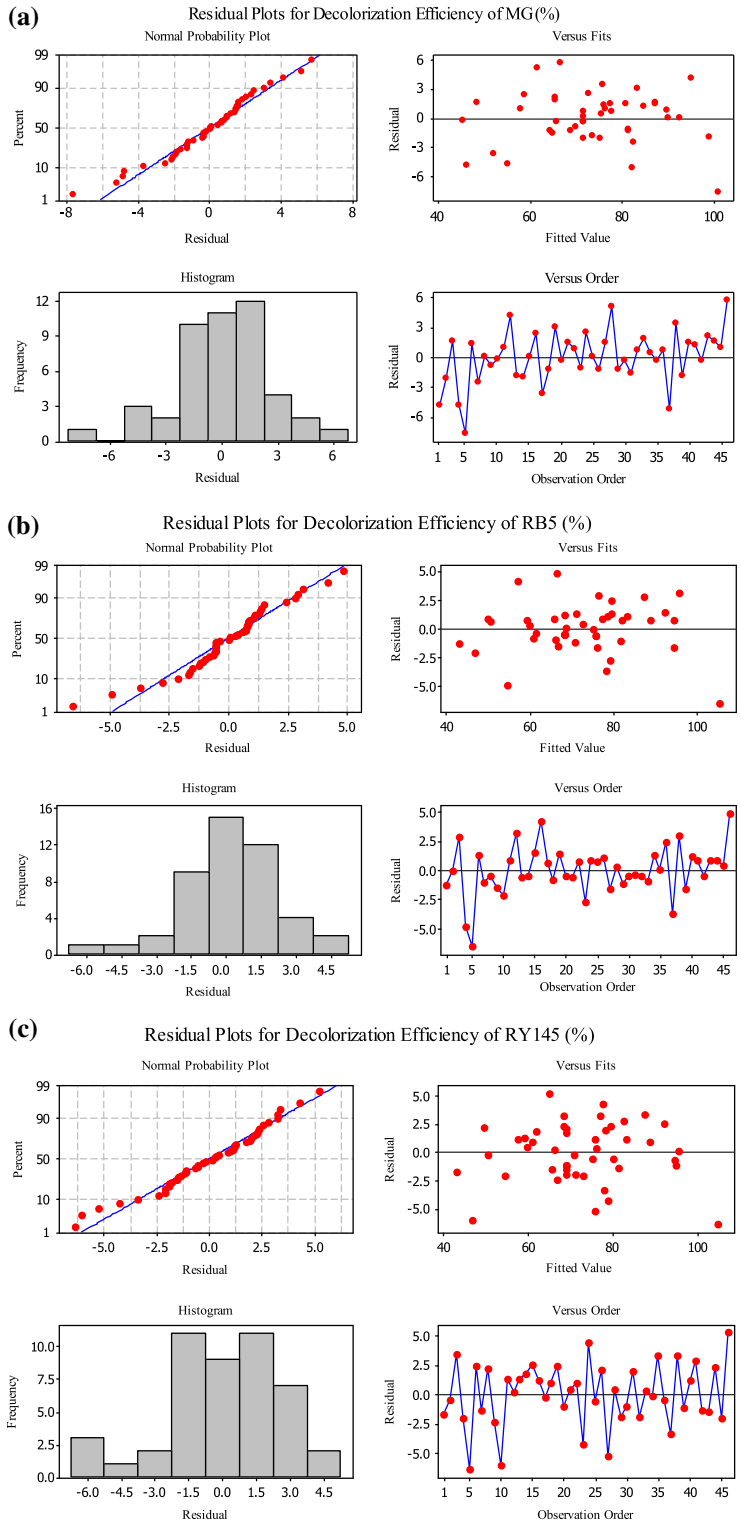


Fig. 2. Anderson–Darling normal distribution graphs. (a) MG, (b) RB5, and (c) RY145.

BBD was set to state decolorization efficiency clearly and Eqs. (16)–(18) were derived as the MNLR models of BBD (Table 4). Explanatory variables of $x_1$, $x_2$, $x_3$, $x_4$, and $x_5$ correspond to temperature, initial pH, reaction time, ultrasonic power, and ozone concentration, response variables of predicted decolorization

efficiencies of $Y_1$, $Y_2$, and $Y_3$ correspond to MG, RB5, and RY145, respectively (Table 5). Furthermore, significant quadratic effects and interactions were found between explanatory variables on response variable in MNLR models of BBD. Adjusted determination coefficient ($R^2_{adj}$) explains the variation in response variable and cross-validated determination coefficient ($R^2_{CV}$) shows the validation between actual values and coded values [25]. VIF greater than 10 shows that there is moderate multicollineerity, and D–W statistics between 0 and 2 means that there is no autocorrelation [26]; quite small value of Press means model has a

Table 5
ANOVA results of BBD

| MG | Source | DF | Seq SS | Adj SS | Adj MS | $F$ | $p$ | VIF | |
|---|---|---|---|---|---|---|---|---|---|
| | Regression | 20 | 8170.72 | 8170.72 | 408.54 | 68.15 | 0.001 | | $R^2 = 0.9610$ |
| | | | | | | | | | $R^2_{adj} = 0.9301$ |
| | $x_1$ | 1 | 327.88 | 327.88 | 327.88 | 54.69 | 0.001 | 84.261 | $R^2_{pred} = 0.8102$ |
| | | | | | | | | | S = 3.54 |
| | $x_2$ | 1 | 3512.04 | 3512.04 | 3512.04 | 585.84 | 0.001 | 78.488 | PRESS = 1537.95 |
| | $x_3$ | 1 | 354.66 | 354.66 | 354.66 | 59.16 | 0.001 | 86.061 | D–W = 1.88 |
| | $x_4$ | 1 | 1075.07 | 902.87 | 902.87 | 150.61 | 0.001 | 93.784 | |
| | $x_5$ | 1 | 187.8 | 114.76 | 114.76 | 19.14 | 0.001 | 85.584 | |
| | $x_1^2$ | 1 | 22.8 | 32.02 | 32.02 | 5.34 | 0.029 | 29.781 | |
| | $x_2^2$ | 1 | 53.19 | 53.19 | 53.19 | 8.87 | 0.006 | 22.172 | |
| | $x_2x_3$ | 1 | 64.88 | 64.88 | 64.88 | 10.82 | 0.003 | 25.447 | |
| | $x_2x_4$ | 1 | 86.12 | 86.12 | 86.12 | 14.37 | 0.001 | 20.282 | |
| | $x_2x_5$ | 1 | 599.03 | 599.03 | 599.03 | 99.92 | 0.001 | 29.089 | |
| | $x_3x_4$ | 1 | 1132.66 | 1132.66 | 1132.66 | 188.94 | 0.001 | 23.697 | |
| | $x_3x_5$ | 1 | 117.94 | 117.94 | 117.94 | 19.67 | 0.001 | 33 | |
| | Regression | 20 | 8243.05 | 8243.05 | 412.15 | 18.79 | 0.001 | | |
| RB5 | $x_1$ | 1 | 113.32 | 113.32 | 113.32 | 5.17 | 0.001 | 84.261 | $R^2 = 0.9760$ |
| | $x_2$ | 1 | 327.88 | 327.88 | 327.88 | 14.95 | 0.001 | 78.488 | $R^2_{adj} = 0.9570$ |
| | $x_3$ | 1 | 3601.5 | 3601.5 | 3601.5 | 164.18 | 0.001 | 86.061 | $R^2_{pred} = 0.8825$ |
| | $x_4$ | 1 | 423.64 | 423.64 | 423.64 | 19.31 | 0.021 | 93.784 | S = 2.81 |
| | $x_5$ | 1 | 884.18 | 701.36 | 701.36 | 31.97 | 0.001 | 85.584 | PRESS = 966.43 |
| | $x_1^2$ | 1 | 266.21 | 183.3 | 183.3 | 8.36 | 0.001 | 29.781 | D–W = 1.98 |
| | $x_2^2$ | 1 | 599.03 | 599.03 | 599.03 | 27.31 | 0.001 | 22.172 | |
| | $x_3^2$ | 1 | 1271.28 | 1271.28 | 1271.28 | 57.95 | 0.015 | 31.417 | |
| | $x_5^2$ | 1 | 380.84 | 380.84 | 380.84 | 17.36 | 0.017 | 30.427 | |
| | $x_1x_4$ | 1 | 113.32 | 113.32 | 113.32 | 5.17 | 0.032 | 21.424 | |
| | $x_2x_3$ | 1 | 327.88 | 327.88 | 327.88 | 14.95 | 0.001 | 25.447 | |
| | $x_2x_5$ | 1 | 3601.5 | 3601.5 | 3601.5 | 164.18 | 0.001 | 29.089 | |
| | $x_3x_4$ | 1 | 423.64 | 423.64 | 423.64 | 19.31 | 0.007 | 23.697 | |
| | $x_3x_5$ | 1 | 884.18 | 701.36 | 701.36 | 31.97 | 0.001 | 33.001 | |
| | Regression | 20 | 7979.56 | 7979.56 | 398.98 | 79.6 | 0.002 | | |
| RY145 | $x_1$ | 1 | 131.22 | 131.22 | 131.22 | 26.18 | 0.001 | 84.261 | $R^2 = 0.9630$ |
| | $x_2$ | 1 | 293.44 | 293.44 | 293.44 | 58.55 | 0.001 | 78.488 | $R^2_{adj} = 0.9340$ |
| | $x_3$ | 1 | 3311.14 | 3311.14 | 3311.14 | 660.64 | 0.001 | 86.061 | $R^2_{pred} = 0.8187$ |
| | $x_4$ | 1 | 456.89 | 456.89 | 456.89 | 91.16 | 0.026 | 93.784 | S = 3.49 |
| | $x_5$ | 1 | 1058.19 | 818.08 | 818.08 | 163.23 | 0.001 | 85.584 | PRESS = 1508.16 |
| | $x_1^2$ | 1 | 260.4 | 191.4 | 191.4 | 38.19 | 0.001 | 29.781 | D–W = 2.45 |
| | $x_2^2$ | 1 | 42.64 | 42.64 | 42.64 | 8.51 | 0.001 | 22.172 | |
| | $x_2x_3$ | 1 | 717.17 | 717.17 | 717.17 | 143.09 | 0.001 | 25.447 | |
| | $x_2x_5$ | 1 | 66.59 | 66.59 | 66.59 | 13.29 | 0.001 | 29.089 | |
| | $x_3x_4$ | 1 | 1138.39 | 1138.39 | 1138.39 | 227.13 | 0.019 | 23.697 | |
| | $x_3x_5$ | 1 | 118.05 | 118.05 | 118.05 | 23.55 | 0.001 | 33.001 | |

Table 6
Results of Tukey's multiple comparison (at a confidence interval of 95%)

| Explanatory variables | | | | Means of | | |
|---|---|---|---|---|---|---|
| Coded | Coded levels | Incoded | Incoded levels | MG | RB5 | RY145 |
| $x_1$ | − | T (°C) | 20 | 69.0 $^{A}$ | 61.1 $^{A}$ | 65.1 $^{A}$ |
| | 0 | | 40 | 74.6 $^{B}$ | 70.0 $^{B}$ | 72.4 $^{B}$ |
| | + | | 60 | 80.1 $^{C}$ | 75.6 $^{C}$ | 77.6 $^{C}$ |
| $x_2$ | − | pH | 2.0 | 81.1 $^{A}$ | 71.1 $^{A}$ | 76.1 $^{A}$ |
| | 0 | | 5.0 | 73.2 $^{B}$ | 66.2 $^{B}$ | 69.2 $^{B}$ |
| | + | | 8.0 | 68.1 $^{C}$ | 61.1 $^{C}$ | 64.4 $^{C}$ |
| $x_3$ | − | RT (min) | 10 | 61. 6 $^{A}$ | 51. 6 $^{A}$ | 56. 6 $^{A}$ |
| | 0 | | 20 | 74.5 $^{B}$ | 64.5 $^{B}$ | 70.5 $^{B}$ |
| | + | | 30 | 91. 2 $^{C}$ | 85. 2 $^{C}$ | 89. 2 $^{C}$ |
| $x_4$ | − | UP (W) | 86 | 75.3 $^{A}$ | 67.3 $^{A}$ | 70.9 $^{A}$ |
| | 0 | | 172 | 70. 1 $^{B}$ | 59. 1 $^{B}$ | 65. 8 $^{B}$ |
| | + | | 344 | 64.4 $^{C}$ | 52.4 $^{C}$ | 57.1 $^{C}$ |
| $x_5$ | − | OC (g/L) | 0.05 | 61.9 $^{A}$ | 51.2 $^{A}$ | 56.9 $^{A}$ |
| | 0 | | 0.10 | 74.1 $^{B}$ | 64.8 $^{B}$ | 69.1 $^{B}$ |
| | + | | 0.15 | 81.3 $^{C}$ | 70.7 $^{C}$ | 75.3 $^{C}$ |

Note: Means do not share the same letter are significantly different.

better predictive ability and a small value of standard error (S) is more precise for the estimated mean response [26,27]. Also Tukey multiple comparisons (95% confidence) was used to state the significat differences between explanatory variables and results of BBD showed that all of explanatory variables had significant differences between factor's levels (Table 6).

### 3.2. Effect of initial pH and reaction time on decolorization efficiency

The increase in reaction time and decrease in initial pH resulted in enhanced decolorization efficiency for all dyes [12,13]. The negative effect of interaction between initial pH and reaction time on decolorization efficiency of MG, RB5, and RY145 standed out (Fig. 3). This stated the importance of initial pH and its effect on ion equilibrium in the mixture medium. Effect of initial pH on decolorization efficiency depends on isoelectric point ($pH_{IEP}$) of dye stuffs [4]. $pH_{IEP}$ of MG, RB5, and RY145 were measured at 1.7, 2.9, and 3.2, respectively. The dyestuff gets negatively charged with pH values above 3.5, thus serving as a repulsive force between the dye and the negatively charged $OH^-$ radicals. Decolorization efficiency was reported to increase when the initial pH of reactive dye solution was set in a range from 1.5 to 3.0 which was attributed to the strongly electrostatic attraction force between radicals and dyestuff [4,12,13]. Similarly, it was stated an increase in decolorization efficiency with decreasing pH from 9 to 5 [4].

### 3.3. Effect of initial pH and ozone concentration on decolorization efficiency

It was reported that decreasing initial pH had a negative effect on decolorization efficiency (Fig. 3). Another negative effect of decreasing initial pH is illustrated in Fig. 4. Fig. 4 also shows the interactive effects of ozone concentration and initial pH on decolorization efficiency. As mentioned before, low frequency ultrasound-assisted ozone process is ozone direct oxidation process in lower pH, so acidic initial pH combined with low concentration of ozone might reach the highest decolorization efficiency (see Eqs. (3)–(10)). Similarly, the same significant interaction on decolorization efficiency between ozone concentration and initial pH of mixture medium was already reported [24,28–30]. On the other hand, further powerful diriving force occured when the initial pH of mixture medium was adjusted to lower than 3.0 [4,7]. Therefore, radical groups of reactive dyestuff can easily react with $O_3$ and this leads to an increase in decolorization efficiency by help of ultrasonic irradiation [4,24,30].

### 3.4. Effect of reaction time and ultrasonic power on decolorization efficiency

Many wastewater treatment processes have been in a positive correlation with increasing reaction time [29–34]. Fig. 5 shows the positive significant effect of increasing reaction time on decolorization efficiency of MG, RB5, and RY145. The interaction between reaction

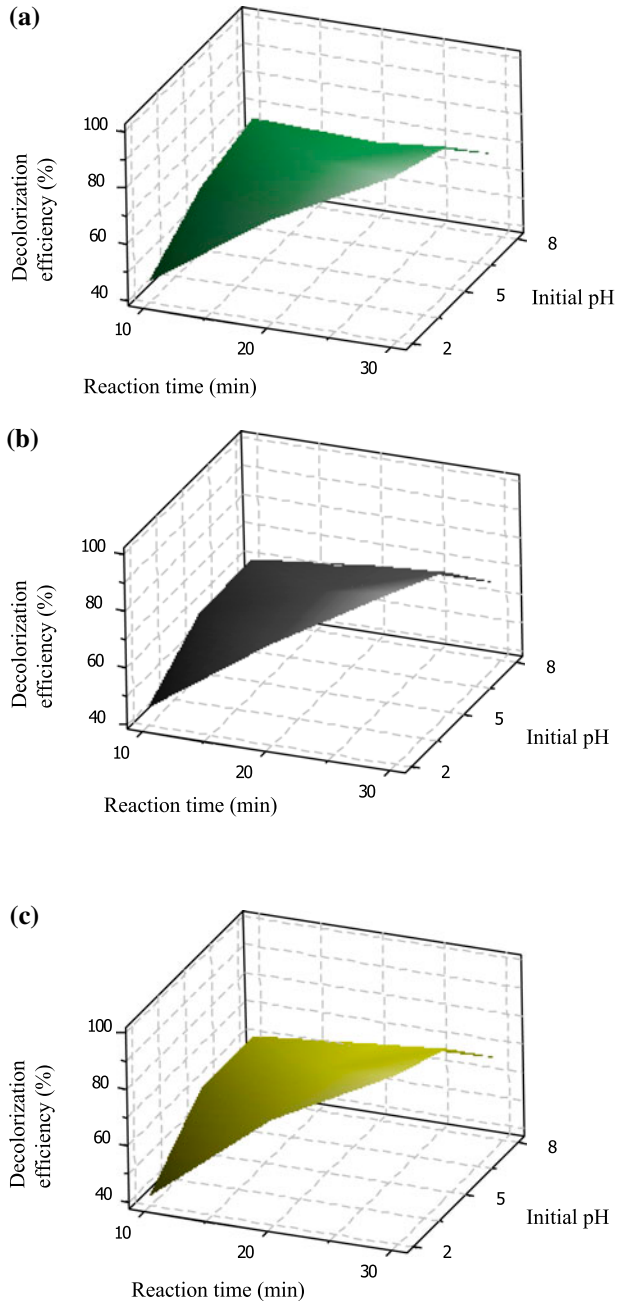


Fig. 3. Response surface 3D plot of effect of initial pH and reaction time on decolorization efficiency (temperature of 40°C, ultrasonic power of 172 W and ozone concentration of 0.10 g/L). (a) MG, (b) RB5, and (c) RY145.

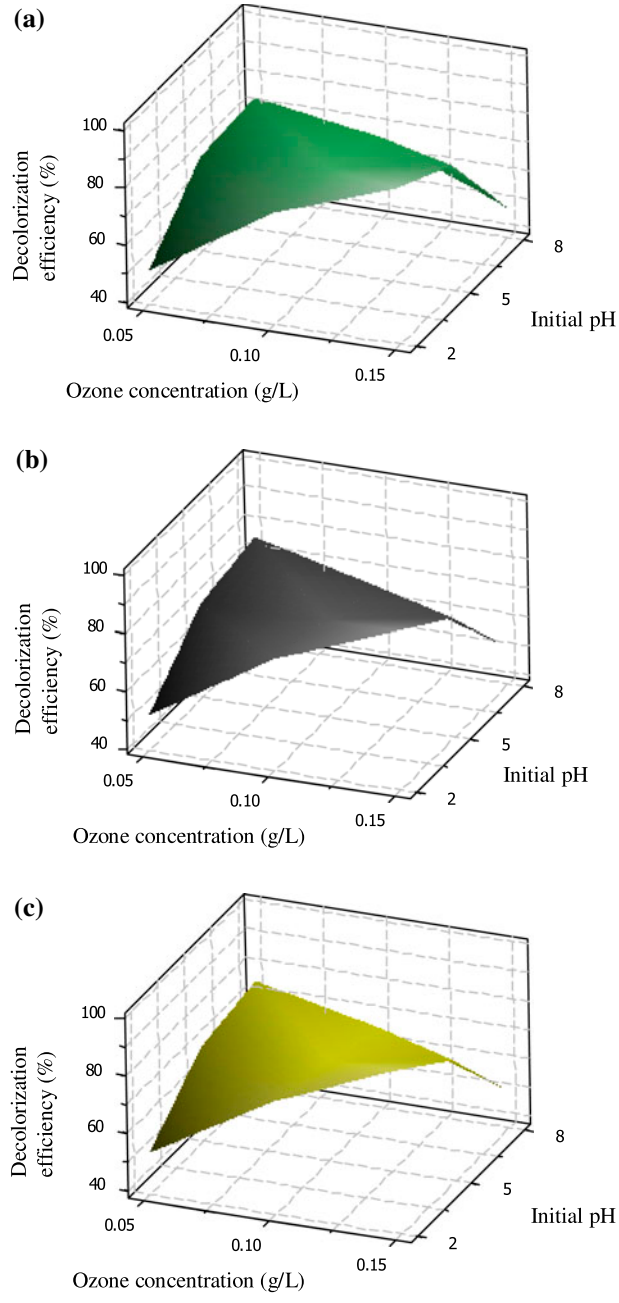


Fig. 4. Response surface 3D plot of effect of initial pH and ozone concentration on decolorization efficiency (temperature of 40°C, reaction time of 20 min, and ultrasonic power of 172 W). (a) MG, (b) RB5, and (c) RY145.

time and ultrasonic power negatively affected decolorization efficiency for all of dyestuffs (Fig. 5). It was stated that ultrasound had both chemical and physical effects on heterogeneous process [28,29]. One of chemical effects of cavitation causes high temperature and pressure and this leads to a thermal decomposition of water into $OH^-$ and $H^+$ [28,33,34]. Instead of increasing decolorization efficiency by increasing reaction time, ultrasonic power, and their interaction have a negative effect on decolorization efficiency. As in the present study, the same positive relationship between reaction time and decolorization

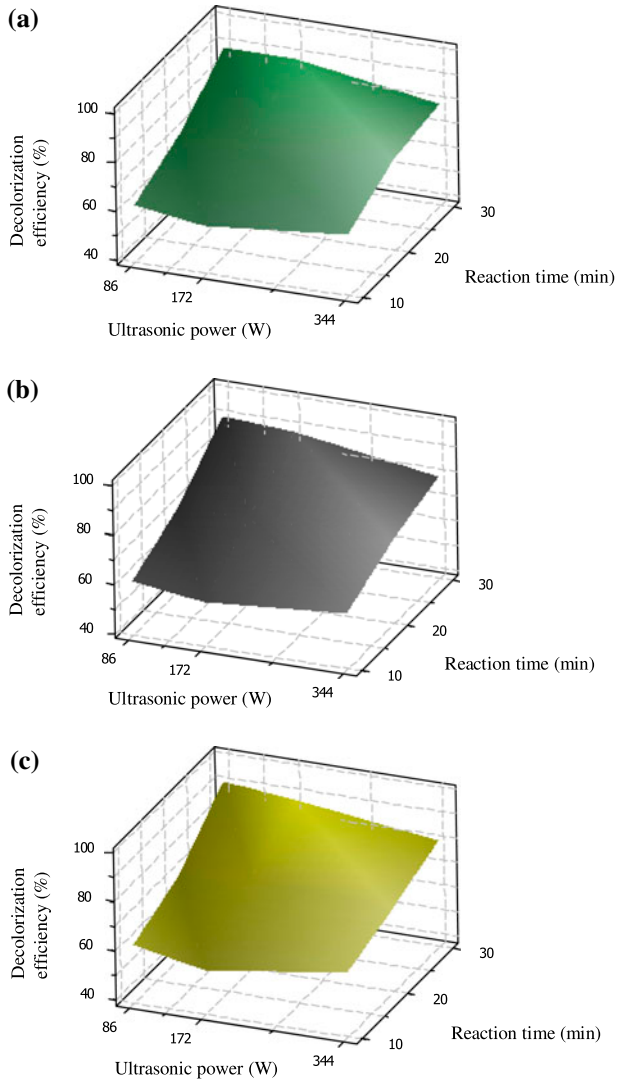


Fig. 5. Response surface 3D plot of effect of reaction time and ultrasonic power on decolorization efficiency (temperature of 40˚C, pH of 5.0 min, and ozone concentration of 0.10 g/L). (a) MG, (b) RB5, and (c) RY145

efficiency was found based on the best-fit MNLR models [1,12,13,29,32–34]. Similarly, it was reported that there is an increase in decolorization efficiency by increasing temperature and reaction time in ultrasound-assisted adsorption process [9] and a 94% decolorization efficiency was obtained based on the adsorption of Chemazol RR195 on dehydrated beet pulp carbon [31].

### 3.5. Effect of reaction time and ozone concentration on decolorization efficiency

Positive effects of increasing reaction time and ozone concentration were clearly defined in previous sections. It was obvious that the longer reaction time further sufficient reaction was going on. Increasing temperature leads to an increase in reacting dyestuff also ultrasonic irradiation increases the temperature of mixture medium as a result of sudden microbubbles collapse. It was stated that color removal rate increases when reaction time increases in ultrasound-assisted ozone oxidation process and a 98.6% decolorization efficiency was reported for the triphenylmethane dyes wastewater using ultrasonic-assisted ozone oxidation under the optimal conditions of 39.8 ˚C, and initial pH 5.2 [12,24]. According to the analysis done above,

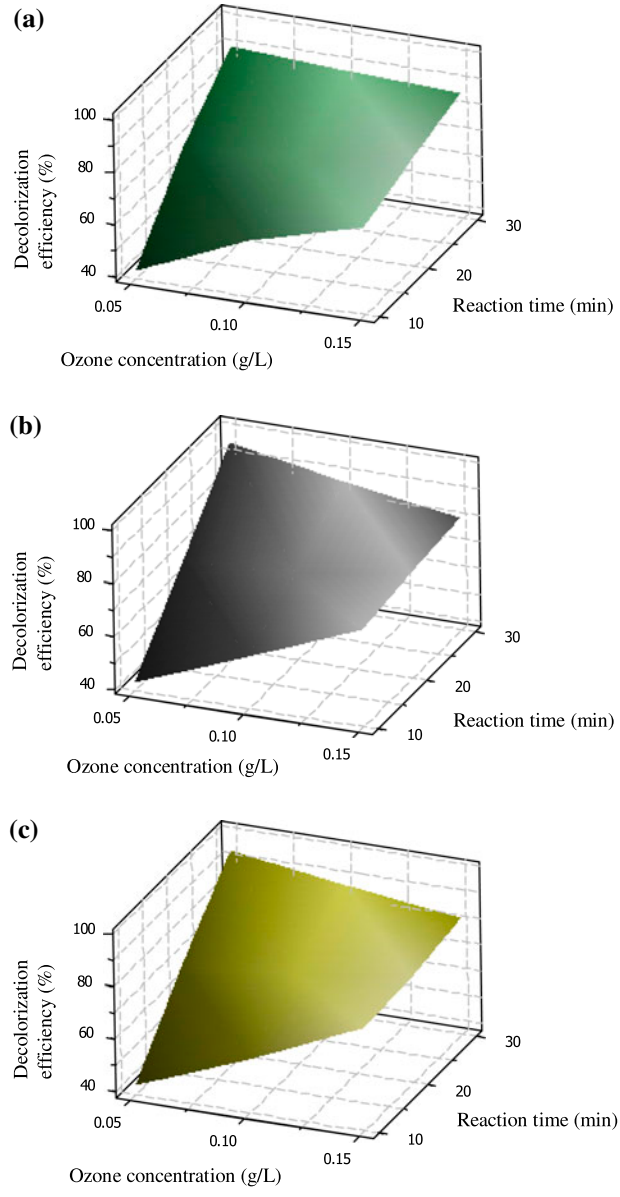


Fig. 6. Response surface 3D plot of effect of reaction time and ozone concentration on decolorization efficiency (temperature of 40˚C, pH of 5.0, and ultrasonic power of 172 W). (a) MG, (b) RB5, and (c) RY145

Table 7
Comparison of decolorization efficiency of ultrasound-assisted ozonation process to different processes

| Decolorization process | Dyestuff | Initial dye concentration (mg/L) | Reaction time (min) | Decolorization efficiency (%) | References |
|---|---|---|---|---|---|
| Ultrasonic irradiation | RB5 | 132 | 17 | 36 | [1] |
| UAOO | MG | 1,000 | 10 | 99.99 | [12] |
| UAO | MO | 400 | 20 | 99 | [22] |
| Ozonation | MG | 662.48 | 20 | 99.99 | [23] |
| UAOO | MG | 1,000 | 10 | 99 | [24] |
| UAO | MG | 1,000 | 30 | 99.31 | This study |
| | RB5 | 1,000 | 30 | 99.86 | |
| | RY145 | 1,000 | 30 | 99.52 | |

Notes: MO: Methyl orange, RB19: Reactive Blue 19, UAA: Ultrasound-assisted adsorption, UAO: Ultrasound-assisted ozonation, and UAOO: Ultrasound-assisted ozone oxidation.

primary mechanism of decolorization was ozone molecule direct oxidation. So, more ozone input leads decolorization efficiency to increase and leads reaction to complete more quickly. Therefore, increased ozone concentration and longer reaction time enhanced decolorization efficiency (Fig. 6).

### 3.6. Comparison UAO with the other methods

Ultrasound-assisted ozonation (UAO) as a rapid and efficient decolorization process was compared to traditional processes and other based on US and/or $O_3$. Unequivocally, it might be seen that UAO seems one of most effective kind of decolorization processes (Table 7). Although high operating cost, attraction of UAO process is further perceptible when decolorization efficiency is explicated. Especially, ultrasonic irradiation leads decolorization efficiency to increase.

## 4. Conclusion

Ultrasound-assisted ozonation excels at decolorization efficiency compared to the other process types owing to its higher decolorization efficiency. The lowest initial pH (2.0), the highest reaction time (30 min), and the highest ozone concentration (0.15 g/L) yielded the highest decolorization efficiency of 99.31, 99.86, and 99.52% for MG, RB5, and RY145, respectively. Initial pH, reaction time, ultrasonic power and ozone concentration, their quadratic terms, and their double interactions were retained in all the best-fit MNLR models as the most significant predictors in accounting for variation in decolorization efficiency. Also, temperature was found to be significantly effective on decolorization efficiency considering liner and quadratic terms in MNLR models.

For future studies, catalytic ozone oxidation, pulsed electric field, or electro-Fenton applications may be applied to decolorization processes in the presence and absence of ultrasonic irradiation to wastewater remains to be explored in terms of economic feasibility and environmental toxicity, and kinetic and thermodynamic parameters of UAO process may be analyzed.

## Acknowledgments

The author would like to thank Dr G.A. Evrendilek for her help with laboratory analysis under her supervision of YENIGIDAM project financially supported by the Turkish State Planning Organization (DPT 2009 K 120 410).

## References

[1] E. Şayan, M.E. Edecan, An optimization study using response surface methods on the decolorization of Reactive Blue 19 from aqueous solution by ultrasound, Ultrason. Sonochem. 15 (2008) 530–538.
[2] M.S. Tanyildizi, Modeling of adsorption isotherms and kinetics of reactive dye from aqueous solution by peanut hull, Chem. Eng. J. 168 (2011) 1234–1240.
[3] E. Şayan, Optimization and modelling of decolorization and COD reduction of reactive dye solutions by ultrasound-assisted adsorption, Chem. Eng. J. 119 (2006) 175–181.
[4] A.R. Dincer, Y. Gunes, N. Karakaya, E. Gunes, Coal-based bottom ash (CBBA) waste material as adsorbent for removal of textile dyestuffs from aqueous solution, J. Hazard. Mater. 141 (2007) 529–535.
[5] S.S. Yang, W.Q. Guo, X.J. Zhou, Z.H. Meng, B. Liu, N.Q. Ren, Optimization of operating parameters for sludge process reduction under alternating aerobic/oxygen-limited conditions by response surface methodology, Bioresour. Technol. 102 (2011) 9843–9851.

[6] S. Song, J. Fan, Z. He, L. Zhan, Z. Liu, J. Chen, X. Xu, Electrochemical degradation of azo dye C.I. Reactive Red 195 by anionic oxidation on $Ti/SnO_2$–$Sb/PbO_2$ electrodes, Electrochim. Acta 55 (2010) 3606–3613.
[7] S. Sahinkaya, COD and color removal from synthetic textile wastewater by ultrasound assisted electro-Fenton oxidation process, J. Hazard. Mater. 19 (2013) 601–605.
[8] A.T. Onat, T.H. Gümüşdere, A. Güvenç, G. Dönmez, U. Mehmetoğlu, Decolorization of textile azo dyes by ultrasonication and microbial removal, Desalination 255 (2010) 154–158.
[9] O. Hamdaoui, M. Chiha, E. Naffrechoux, Ultrasound-assisted removal of malachite green from aqueous solution by dead pine needles, Ultrason. Sonochem. 15 (2008) 799–807.
[10] O. Gulnaz, A. Kaya, S. Dincer, The reuse of dried activated sludge for adsorption of reactive dye, J. Hazard. Mater. 134 (2006) 190–196.
[11] D. Özer, G. Dursun, Methylene blue adsorption from aqueous solution by dehydrated peanut hull, J. Hazard. Mater. 144 (2007) 171–179.
[12] X.J. Zhou, W.Q. Guo, S.S. Yang, N.Q. Ren, A rapid and low energy consumption method to decolorize the high concentration triphenylmethane dye wastewater: Operational parameters optimization for the ultrasonic-assisted ozone oxidation process, Bioresour. Technol. 105 (2012) 40–47.
[13] X.J. Zhou, W.Q. Guo, S.S. Yang, H.S. Zheng, N.Q. Ren, Ultrasonic-assisted ozone oxidation process of triphenylmethane dye degradation: Evidence for the promotion effects of ultrasonic on malachite gren decolorization and degradation mechanism, Bioresour. Technol. 128 (2013) 827–830.
[14] T. Robinson, G. McMullan, R. Marchant, P. Nigam, Remediation of dyes in textile effluent: A critical review on current treatment technologies with a proposed alternative, Bioresour. Technol. 77 (2001) 247–255.
[15] B.D. Voncina, A. Majcen-Le-Marechal, Reactive dye decolorization using combined ultrasound/$H_2O_2$, Dyes Pigm. 59 (2004) 173–179.
[16] E. Demirbas, M. Kobya, M.T. Sulak, Adsorption kinetics of a basic dye from aqueous solutions onto apricot stone activated carbon, Bioresour. Technol. 99 (2008) 5368–5373.
[17] Y. Li, W.P. Hsieh, R. Mahmudov, X. Wei, C.P. Huang, Combined ultrasound and Fenton (US–Fenton) process for the treatment of ammunition wastewater, J. Hazard. Mater. 244–245 (2013) 403–411.
[18] M.A. Behnajady, N. Modirshahla, M. Shokri, B. Vahid, Effect of operational parameters on degradation of Malachite Green by ultrasonic irradiation, Ultrason. Sonochem. 15 (2008) 1009–1014.
[19] O. Korkut, E. Sayan, O. Lacin, B. Bayrak, Investigation of adsorption and ultrasound assisted desorption of lead(II) and copper(II) on local bentonite: A modelling study, Desalination 259 (2010) 243–248.
[20] W.Q. Guo, J. Ding, G.L. Cao, N.Q. Ren, F.Y. Cui, Treatability study of using low frequency ultrasonic pretreatment to augment continuous biohydrogen production, Int. J. Hydrogen Energy 36 (2011) 14180–14185.
[21] O. Lacin, B. Bayrak, O. Korkut, E. Sayan, Modeling of adsorption and ultrasonic desorption of cadmium(II) and zinc(II) on local bentonite, J. Colloid Interface Sci. 292 (2005) 330–335.
[22] H. Zhang, L. Duan, D. Zhang, Decolorization of methyl orange by ozonation in combination with ultrasonic irradiation, J. Hazard. Mater. 138 (2006) 53–59.
[23] E. Kusvuran, O. Gulnaz, A. Samil, O. Yildirim, Decolorization of malachite gren, decolorization kinetics and stoichiometry of ozone-malachite gren and removal of antibacterial activity with ozonation processes, J. Hazard. Mater. 186 (2011) 133–143.
[24] X.J. Zhou, W.Q. Guo, S.S. Yang, H.S. Zheng, N.Q. Ren, Ultrasonic-assisted ozone oxidation process of tripneylmethane dye degradation: Evidence for the promotion of ultrasonic on malachite gren decolorization and degradation mechanism, Bioresour. Technol. 128 (2013) 827–830.
[25] D.W. Hosmer, S. Lemeshow, Appilied Logistic Regression, second ed., John Wiley & Sons, Inc, 2000,
[26] I.E. Frank, J.H. Friedman, A statistical view of some chemometrics regression tools, Technometrics 35 (1993) 109–135.
[27] P. McCullagh, J.A. Nelder, Generalized Linear Model, Chapman and Hall, London, 1992.
[28] Z. Ai, J. Li, L. Zhang, S. Lee, Rapid decolorization of azo dyes in aqueous solution by an ultrasound-assisted electrocatalytic oxidation proces, Ultrason. Sonochem. 17 (2010) 370–375.
[29] K. Turhan, I. Durukan, S.A. Ozturkcan, Z. Turgut, Decolorization of textile basic dye in aqueous solution by ozone, Dyes Pigm. 92(3) (2012) 897–901.
[30] K. Turhan, S.A. Ozturkcan, Decolorization and degradation of reactive dye in aqueous solution by ozonisation semi-batch bubble column reactor, Water Air Soil Pollut. 224 (2013) 1353–1358.
[31] A.Y. Dursun, O. Tepe, Removal of Chemazol Reactive Red 195 from aqueous solution by dehydrated beet pulp carbon, J. Hazard. Mater. 194 (2011) 303–311.
[32] K. Turhan, Z. Turgut, Treatment and degradability of direct dyes in textile wastewater by ozonation: A laboratory investigation, Desalin. Water Treat. 11(1–3) (2009) 184–191.
[33] C. Wang, A.Yediler, D. Lienert, Z. Wang, A. Kettrup, Ozonation of an azo dye C.I. Remazol Black 5 and toxicological assessment of oxidation products, *Chemosphere* 52 (2003) 1225–1232
[34] W. Chu, C. Ma, Quantitative prediction of direct and indirect dye ozonation kinetics, Water Res. 34(12) (2000) 3153–3160.